Available online at www.sciencedirect.com

SciVerse ScienceDirect

journal homepage: www.elsevier.com/locate/he

Steam reforming of ethanol over Co_3O_4–Fe_2O_3 mixed oxides☆

A. Abdelkader [a,b], H. Daly [a], Y. Saih [a,c], K. Morgan [a], M.A. Mohamed [b], S.A. Halawy [b], C. Hardacre [a,*]

[a] CenTACat, School of Chemistry and Chemical Engineering, Queen's University Belfast, Belfast BT9 5AG, Northern Ireland, UK

[b] Chemistry Department, Faculty of Science, South Valley University, Qena 83523, Egypt

[c] KAUST Catalysis Center, KAUST, Thuwal 23955-6900, Jeddah, Kingdom of Saudi Arabia

ARTICLE INFO

Article history:
Received 7 February 2013
Received in revised form
29 March 2013
Accepted 1 April 2013
Available online 3 May 2013

Keywords:
Steam reforming
Ethanol
Hydrogen
Cobalt–iron catalyst
DRIFTS-MS

ABSTRACT

Co_3O_4, Fe_2O_3 and a mixture of the two oxides Co–Fe (molar ratio of $Co_3O_4/Fe_2O_3 = 0.67$ and atomic ratio of Co/Fe = 1) were prepared by the calcination of cobalt oxalate and/or iron oxalate salts at 500 °C for 2 h in static air using water as a solvent/dispersing agent. The catalysts were studied in the steam reforming of ethanol to investigate the effect of the partial substitution of Co_3O_4 with Fe_2O_3 on the catalytic behaviour. The reforming activity over Fe_2O_3, while initially high, underwent fast deactivation. In comparison, over the Co–Fe catalyst both the H_2 yield and stability were higher than that found over the pure Co_3O_4 or Fe_2O_3 catalysts. DRIFTS-MS studies under the reaction feed highlighted that the Co–Fe catalyst had increased amounts of adsorbed OH/water; similar to Fe_2O_3. Increasing the amount of reactive species (water/OH species) adsorbed on the Co–Fe catalyst surface is proposed to facilitate the steam reforming reaction rather than decomposition reactions reducing by-product formation and providing a higher H_2 yield.

1. Introduction

Currently, there is a significant drive to move away from the use of non-renewable fossil fuels, i.e. petroleum, natural gas and coal, for energy production due to the associated environmental problems such as the production of air pollutants and greenhouse gas emissions [1]. One of the most attractive options to replace fossil fuel derived hydrocarbons is to use hydrogen coupled with, for example, fuel cell technology. Although significant amounts of hydrogen are produced by the steam reforming of natural gas, the production of hydrogen from alternative, sustainable sources is highly desirable with one such process being the steam reforming of bioethanol which is produced via biomass fermentation processes. Due to the potential of this process, the steam reforming of ethanol to produce hydrogen has been widely investigated [2,3].

A wide range of catalysts have been studied for the steam reforming of ethanol including solid oxides, transition metals and noble metals as well as multi metallic catalysts [3]. Although noble metals exhibit high activity and stability towards ethanol steam reforming (ESR), their use is undesirable due to their high cost. For non-noble metal catalysts, Ni and Co have been reported to exhibit the best performance for ethanol steam reforming favouring C–C bond cleavage and a high selectivity for H_2 production [1]. Co-based catalysts have been actively researched for the process as less methane and

* *Corresponding author*. Tel.: +44 28 9097 4592.
E-mail address: c.hardacre@qub.ac.uk (C. Hardacre).

0360-3199/$ – see front matter
http://dx.doi.org/10.1016/j.ijhydene.2013.04.009

more hydrogen is generated compared with Ni-based catalysts. However, the deactivation of Co-based catalysts as a result of sintering and/or carbon deposition over the catalyst surface has hindered the wider use of these catalysts for steam reforming reactions [4]. Consequently, most of the studies investigating cobalt catalysts for ethanol steam reforming have been in the area of improving their activity and, importantly, stability while concomitantly reducing the formation of undesired by-products, in particular coke.

The addition of promoters such as noble metals [5,6], Ni, Cu, Na, Mn, Cr and Fe [4,7–14] to Co catalysts has been investigated for their effect on the activity and stability for ethanol steam reforming. In particular, promotion with Fe has been reported to improve activity and H_2 yield over Co/α-Al_2O_3 and Co/$SrTiO_3$ catalysts [4,14] and Co/ZnO supported catalysts [8]. In the latter, Fe promoted Co/ZnO also exhibited improved water gas shift (WGS) activity at low temperatures. Unsupported Co_3O_4 catalysts have also been reported to be active for steam reforming of ethanol [11,15–18] with 1% Fe doped onto Co_3O_4 also showing a promoting effect with lower CH_4 and CO formed compared to Co_3O_4. In most reports the addition of Fe to Co catalysts enhances the dehydrogenation of ethanol and increases the transformation of acetaldehyde selectively without promoting formation of by-products, such as methane and coke [4,12,14,16]. The promoting effect of Fe has been attributed to the formation of Co–Fe solid solutions [11], Co–Fe alloys [8] and close contact between the Co and Fe (no new phases detected) [14]. The interaction between the Co and Fe in the catalysts is likely related to the preparation method with solid solutions and alloys formed from co-precipitation and co-impregnation methods respectively while close contact was reported for sequential impregnation of Fe onto Co/ZnO catalyst.

In this study, the catalysts have been prepared by a simple, one pot synthesis procedure producing a mixed Co–Fe oxide catalyst (1:1 atomic ratio) following decomposition of the oxalate precursors in air. No solid solution formation is expected from this method [19] hence the promoting effect is expected to result from close contact between separate oxide phases. Contact between the phases is expected to be enhanced with partial substitution of Co with Fe as opposed to doping with Fe. As a reference, a physical mixture of Co_3O_4 and Fe_2O_3 (Co–Fe-Physical) was prepared from grinding together the individual oxides and this catalyst was tested under the same reaction conditions.

2. Experimental

2.1. Catalyst preparation

Pure cobalt oxide (Co_3O_4) and iron oxide (Fe_2O_3) samples were prepared by the calcination of cobalt (II) oxalate dihydrate, $Co(C_2O_4)\cdot 2H_2O$ (Sigma–Aldrich) and iron (II) oxalate dihydrate, $Fe(C_2O_4)\cdot 2H_2O$ (Sigma–Aldrich), respectively. The oxalate samples were calcined for 2 h in static air at 500 °C in a muffle furnace after ramping from room temperature at 5 °C min^{-1}.

The mixed Fe_2O_3 and Co_3O_4 oxide sample (Co–Fe) was prepared using 11.3 g iron (II) oxalate dihydrate, $Fe(C_2O_4)\cdot 2H_2O$ (Sigma–Aldrich) and 11.4 g cobalt (II) oxalate dihydrate, $Co(C_2O_4)\cdot 2H_2O$ (Sigma–Aldrich) dissolved in approximately 10 cm^3 doubly deionised (18 MΩ) water at room temperature until a homogeneous paste was obtained. This paste was dried at 100 °C in an oven for 20 h before being calcined in static air at 500 °C for 2 h after ramping from room temperature at 5 °C min^{-1}. The catalyst obtained contained 40 mol % Co_3O_4 + 60 mol% Fe_2O_3 which gives an atomic ratio of Co/Fe = 1. The physical mixture (Co–Fe-Physical) with the same composition as the Co–Fe sample was prepared by grinding together the calcined Co_3O_4 and Fe_2O_3.

2.2. Characterization techniques

X-ray diffraction was carried out using a PANalytical X'Pert Pro X-ray diffractometer equipped with a Cu K_α X-ray source and the X-ray detector set to 40 kV and 40 mA. Under ambient conditions, a Spinner PW3064 sample stage was used. Identification of the diffraction peaks was undertaken using the PCPDFWIN database.

Temperature programmed reduction (TPR) experiments were performed in a fixed-bed quartz U-tube reactor using 20 mg of the fresh catalyst. The sample was exposed to 5% H_2/Ar (20 cm^3 min^{-1}) and heated from room temperature to 1000 °C at a heating rate of 15 °C min^{-1} and hydrogen consumption (*m/z*: 2) was monitored during the temperature ramp using a Hiden Analytical HPR20 quadrupole mass spectrometer with a capillary inlet.

Temperature programmed oxidation (TPO) measurements were performed to assess the amount of carbon deposited on the catalysts after 2 h of reaction. 50 mg of the used catalyst was ramped from 30 to 800 °C at a heating rate of 10 °C min^{-1} in 5% O_2/Ar (50 cm^3 min^{-1}) while monitoring the evolution of carbon dioxide (*m/z*: 44) and carbon monoxide (*m/z*: 28) using a Hiden Analytical HPR20 quadrupole mass spectrometer with a capillary inlet.

Temperature programmed desorption of ammonia (NH_3-TPD) was obtained from samples (100 mg) pre-reduced using 40 cm^3 min^{-1} of 25% H_2/Ar at 400 °C for 1 h. After cooling to 40 °C in Ar (30 cm^3 min^{-1}), the samples were exposed to 0.4% NH_3/Ar (50 cm^3 min^{-1}) for 2 h and then the sample was flushed with Ar (50 cm^3 min^{-1}) for 30 min. The NH_3-TPD measurements were carried out with a heating rate of 10 °C min^{-1} from 40 to 800 °C under a flow of Ar (50 cm^3 min^{-1}). Desorption of ammonia (*m/z*: 16) was monitored using a Hiden Analytical HPR20 quadrupole mass spectrometer with a capillary inlet.

BET surface area measurements were performed at liquid nitrogen temperature using an automatic ASAP-2010 sorptometer (Micromeritics). The catalyst samples were outgassed at 200 °C for 1 h prior to each measurement.

Transmission electron microscopy (Philips TECNAI F20 Transmission electron microscope) at 200 kV was performed to analyse the morphology of the samples. The catalysts were suspended following ultrasonic agitation for ~2 min in ethanol and the suspension then deposited onto copper grids before the ethanol was evaporated. Elemental analysis of catalyst samples was carried out using EDX on STEM imaging.

Raman analysis, of the fresh catalysts and used catalysts after 15 h of reaction at 500 °C under the ESR feed, was carried out using an Avalon Ramanstation fiberoptic system with a

785 nm laser; spectra were accumulated for 2 min with a resolution of 2 cm^{-1}.

2.3. Catalytic reaction

Before exposure to the reaction feed, the catalyst was heated from room temperature to 400 °C at a heating rate of 10 °C min^{-1}, in Ar at 60 cm^3 min^{-1} followed by reduction for 1 h at 400 °C in 25% H_2/Ar at 80 cm^3 min^{-1}. Following the reduction, the feed was changed to Ar (60 cm^3 min^{-1}) and the temperature ramped from 400 to 500 °C at a heating rate of 10 °C min^{-1}. At 500 °C, the water/ethanol/Kr/Ar feed (mole ratio of 1/3/0.6/11.4) at 80 cm^3 min^{-1} was introduced to the catalyst bed (200 mg of catalyst diluted with 500 mg SiC) held in a quartz reactor (13 mm internal diameter) under atmospheric pressure; Kr was added to the feed as an internal standard for determination of the carbon balance. The liquid water–ethanol mixture was delivered by a syringe-free liquid pump from Valco Instruments Co. Inc. into an evaporator heated at 100 °C. The output gas mixture was analysed on-line by gas chromatography (Clarus 500, PerkinElmer) with TCD and FID (coupled with a methaniser) detectors.

The stoichiometric ethanol steam reforming reaction is shown below (Eq. (1)):

$$CH_3CH_2OH + 3H_2O \rightarrow 2CO_2 + 6H_2 \quad (1)$$

The hydrogen yield (H_2 Y %), ethanol conversion (Ethanol conv. %) and selectivity of carbon-containing products (S %) are defined as:

H_2 Y % = (moles of hydrogen produced × 100)/(6 × moles of ethanol fed)

Ethanol conv. % = (moles of ethanol converted × 100)/(moles of ethanol fed)

S % of product A = (*N* × moles of A produced × 100)/(2 × moles of ethanol converted)

where *N* is the number of carbon atoms in the product A.

2.4. Diffuse reflectance infra-red Fourier transform spectroscopy-mass spectroscopy analysis (DRIFTS-MS)

The DRIFTS setup consisted of an in-situ high temperature diffuse reflectance IR cell (Spectra-Tech) fitted with ZnSe windows which was modified in house to behave as a plug flow reactor [20]. All DRIFT spectra were recorded using a Bruker Vertex 70 spectrometer using an average of 256 scans and a resolution of 4 cm^{-1}. Analysis of the gas from the outlet of the DRIFTS cell was performed with a Hiden Analytical HPR20 quadrupole mass spectrometer (QMS) with a capillary inlet. Reagents and products were monitored by the following *m*/*z* values: 2 (for H_2), 15 (for CH_4), 18 (for H_2O), 26 and 27 (for ethylene), 28 (for CO), 29 (for acetaldehyde), 31 (for ethanol), 43 (for acetone) and 44 (for CO_2).

Prior to reaction, the catalyst (~50 mg) was pre-reduced under 25% H_2/Ar (20 cm^3 min^{-1}) for 1 h at 400 °C. After reduction, the temperature was lowered to 100 °C and the reduced catalyst taken as a background spectrum. A gas feed of 20 cm^3 min^{-1} containing ethanol/water/Kr/Ar (mole ratio of 1/3/0.6/11.4) was fed over the catalyst at 100 °C for 1 h thereafter the temperature was increased to 500 °C at 10 °C min^{-1}. The catalyst was held at 500 °C for 1 h under the reaction feed. The liquid water–ethanol-inert mixture was delivered by a 3-way mixing valve and evaporator (Bronkhorst) with the evaporation temperature held at 100 °C.

3. Results and discussion

3.1. Catalytic behaviour

Co_3O_4, Fe_2O_3, Co–Fe-physical and Co–Fe samples were tested for activity in the steam reforming of ethanol. Fig. 1 shows the %ethanol conversion and %H_2 yield and Table 1 summarises the %selectivity to carbon-containing compounds as a function of time on stream at 500 °C. Fe_2O_3 exhibited some initial activity for the steam reforming of ethanol at 500 °C with a H_2 yield of 60% and selectivity to CO_2 of 36.1% with CO (39.5%) and undetected carbon (23.1%) also formed. The Fe_2O_3 catalyst underwent rapid deactivation with an initial ethanol conversion of 90% after 0.75 h on stream dropping to 10% after 6 h of reaction. While initial activity for the steam reforming of ethanol (H_2 and CO_2 formation) was observed, with time on stream, the H_2 yield decreased more rapidly than the ethanol conversion with an increase in the selectivity towards acetaldehyde. In addition, no methane was observed over this

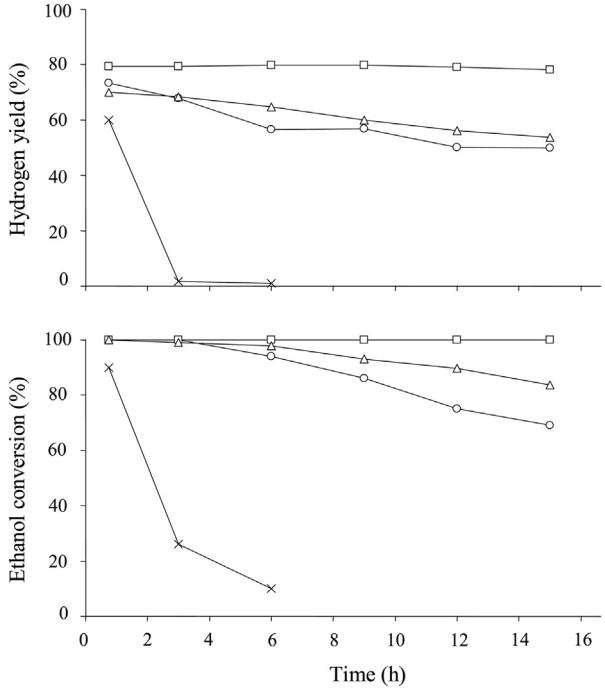

Fig. 1 – %Ethanol conversion and % hydrogen yield as a function of reaction time in ethanol steam reforming over Co_3O_4 (○), Co–Fe-physical (△), Co–Fe (□) and Fe_2O_3 (×) at 500 °C, ethanol:water = 1:3, 200 mg catalyst and a total flow of 80 cm^3 min^{-1}.

Table 1 – %Selectivity to carbon-containing products in the ethanol steam reforming over the Fe_2O_3, Co_3O_4, Co–Fe-Physical and Co–Fe catalysts as a function of time on stream at 500 °C, ethanol/:water = 1:3, 200 mg catalyst and a total flow of 80 cm^3 min^{-1}.

Catalyst	Time on Stream (h)	CO_2	CO	CH_4	CH_2CH_2	CH_3CHO	Undetected carbon
Fe_2O_3	0.75	36.1	39.5	0	1	0.3	23.1
	3	3.2	3.6	0	8.5	83.2	1.5
	6	4	4	0	8.7	83	0.3
Co_3O_4	0.75	42.1	18.3	10.7	0	0.1	28.8
	3	40	18.9	10.7	0	0.7	29.7
	6	38.1	19.3	10.7	0	1.6	30.3
	9	38.6	19	10.5	0	2.3	29.6
	12	41.3	18.2	10.1	0	2.9	27.5
	15	45	17.4	9.8	0	3.3	24.5
Co–Fe-physical	0.75	35.6	37.4	7.1	0	3.3	16.6
	3	36.4	36.2	6.8	0	5.2	15.4
	6	37	34.7	5.9	0	8.1	14.3
	9	37.8	32.5	5.3	0	10.9	13.5
	12	39.5	29.3	4.9	0	13.3	13
	15	42.3	25.4	4.6	0	15.2	12.5
Co–Fe	0.75	49	39	4	0	1.3	6.7
	3	49.7	38.5	3.9	0	1.1	6.8
	6	50.5	37.7	3.8	0	0.7	7.3
	9	51.1	36.5	3.6	0	0.3	8.5
	12	50.9	35.7	3.6	0	0.2	9.6
	15	50.3	35.3	3.7	0	0.4	10.3

catalyst indicating that little acetaldehyde (or ethanol) decomposition occurred.

Co_3O_4 was more active than Fe_2O_3 with a H_2 yield of 73% at 100% conversion of ethanol. This catalyst also deactivated with time on stream although at a slower rate than that found for Fe_2O_3. The %selectivity towards C1 vs C2 products over the Co_3O_4 catalyst demonstrated that this catalyst has higher activity for C–C bond breaking compared with Fe_2O_3 with initial %selectivity to CO_2, CO and CH_4 considerable higher than acetaldehyde with no ethylene formation observed at 500 °C. While no ethylene in the gas phase was observed over Co_3O_4, the selectivity to undetected carbon was higher than over the Fe_2O_3 catalyst which suggests that over the Co_3O_4 catalyst coke deposition could be the cause of the deactivation.

The physical mixture of Co_3O_4 and Fe_2O_3, while also exhibiting initial complete conversion of ethanol (as for the Co_3O_4 catalyst) importantly showed a lower selectivity to undetected carbon compared with either of the two pure oxides, in addition a decrease in CH_4 formation was also observed. Ethanol conversion over the physically mixed catalyst decreased at a slower rate compared to over the Co_3O_4 catalyst while the $\%H_2$ yield was found to decrease at a similar rate over both catalysts. As there was no promotional effect on the pathways for H_2 production from physically mixing the two oxides, this suggests that these reactions occur over the Co_3O_4. However, contact between the two oxides did provide a synergetic effect in terms of reducing by-product formation (both methane and coke).

The Co–Fe sample, which was prepared from static air calcination of an aqueous paste of Co and Fe oxalate precursors, exhibited the highest hydrogen yield (80%) and greater selectivity to CO_2 and CO compared with the pure oxides and the physical mixture. Addition of Fe_2O_3 to the Co_3O_4 catalyst was also observed to lower the selectivity to methane and undetected carbon by-products over and above the enhancement found for the physical mixture. The average value for the selectivity to undetected carbon was 8.2% for Co–Fe compared with 28.5% for Co_3O_4 and 14.3% for the physical mixture.

A comparison of the ethanol steam reforming activity over Co/Al_2O_3, Fe/Al_2O_3 and a physical mixture of the two catalysts was reported by Kazama et al. [14]. Therein, it was shown that Co/Al_2O_3 was more active with respect to ethanol conversion and more stable and had higher H_2 and CO_2 yields compared with the Fe/Al_2O_3 catalyst which exhibited low ethanol conversion and low H_2 yield with fast deactivation over 3 h of reaction at 550 °C. This is comparable to the results obtained over the Fe_2O_3 catalyst in this study where fast deactivation was observed. As found for the unsupported Fe_2O_3, the supported Fe catalyst also showed increased selectivity to acetaldehyde as the catalyst deactivated. In contrast with the present study, the physical mixture of Co/Al_2O_3 and Fe/Al_2O_3 exhibited higher ethanol conversion and higher H_2 yields compared with the individual Co/Al_2O_3 and Fe/Al_2O_3 catalysts showing a clear promotion of Fe on the activity of the Co-based catalyst [14].

Promotion of Co_3O_4 catalysts with Fe has also been reported by de la Pena et al. [11]. Using a reaction temperature of 400 °C and an ethanol: water ratio of 1:6, Co_3O_4 doped with 1 wt% Fe and Fe incorporation into the Co_3O_4 spinel structure forming a solid solution ($Fe_xCo_{3-x}O_4$ with $0 < x < 0.60$) exhibited enhanced H_2 selectivities and low CO and CH_4 formation. The concentration of Fe incorporated into the solid solution affected the activity and selectivity of the reaction

with Fe ≥ 0.15 showing lower ethanol conversion and higher selectivities towards acetaldehyde. High selectivity for acetaldehyde was also observed over pure Fe/Al_2O_3 [14] and Fe_2O_3 catalysts in this work. Of interest is that in the catalyst preparation [11], NaOH was used as the precipitating agent with appreciable amounts (compared with the Fe content) of Na detected on the catalysts. Na has been reported to be a promoter for Co catalysts reducing coke formation possibly having an additional effect on these catalysts [21].

3.2. *Characterization of catalysts*

Fig. 2 shows the XRD diffraction patterns of Co_3O_4, Fe_2O_3, Co–Fe-Physical and Co–Fe samples. The Co_3O_4 sample is consistent with the cubic structure of Co_3O_4 (PDF-#: 76-1802) [22] while the Fe_2O_3 sample shows hematite to be the main crystalline phase (PDF-#: 89-0599) [23]. Both the physical mixture (Co–Fe-Physical) and the mixed oxide sample Co–Fe, contained peaks due to both Fe_2O_3 hematite and cubic Co_3O_4. No other phases/shift in peak positions were observed by XRD in this study which suggests that no extensive solid solution was formed between the two oxides as a result of this preparation method. However, low concentration of solid solution formation cannot be discounted as for a Co/ZnO catalyst promoted with 1% Fe, XRD did not identify any different phases yet cobalt–iron alloy formation was observed from HRTEM and EELS techniques [7,8]. However, Gabal et al. characterised the cobalt and iron phases in a cobalt–iron oxalate mixture with calcination temperature and showed that, after the initial dehydration, decomposition of $FeC_2O_4 \cdot 2H_2O$ was followed by decomposition of $CoC_2O_4 \cdot 2H_2O$ to form Co_3O_4–Fe_2O_3 by 265 °C with Co_3O_4–Fe_2O_3 being thermally stable up to 920 °C. Of relevance to this study, a solid solution, $CoFe_2O_4$, was only detected at calcination temperatures of 1000 °C [19], therefore, using the preparation method described, herein (mixing the respective oxalates in water at room temperature followed by calcination in air at 500 °C) a solid solution is not expected to form between Co and Fe.

Fig. 3 shows TEM images of Co_3O_4, Fe_2O_3, Co–Fe-Physical and Co–Fe samples. The average particle size of the Co_3O_4 catalyst (Fig. 3A) was 10–50 nm which is smaller than that of the Fe_2O_3 catalyst, 50–150 nm (Fig. 3B). The size difference between the particles is clear in the micrograph of the Co–Fe-Physical sample (Fig. 3C), where the size of the individual Fe_2O_3 and Co_3O_4 particles in the physical mixture are comparable to that measured for the pure oxide samples despite the catalyst being prepared by grinding together the two oxides. EDX analysis of the particles in the physical mixture confirmed that the larger particles contained only Fe and the smaller particles contained only Co. For the Co–Fe sample, (Fig. 3D) the particle size was in the range of 10–50 nm, which was similar to the particle size of the pure Co_3O_4 catalyst. However, it was not possible to distinguish (by EDX) separate particles of Fe_2O_3 or Co_3O_4 in contrast with the physical mixture. This demonstrates that while separate phases are shown by the XRD, the two phases are in intimate contact within a given particle rather than the oxides forming separate distinct particles. These results indicate that grinding the two oxides together as in the Co–Fe-Physical sample, while providing some improvement in selectivity, does not form the same degree of contact between the two oxides as observed in the Co–Fe sample which results in a more significant reduction in by-product formation. In addition to greater contact between the oxides in the Co–Fe sample, the surface area was also increased substantially from 18 $m^2\ g^{-1}$ for Co_3O_4 and 13.5 $m^2\ g^{-1}$ for Fe_2O_3 to 29.3 $m^2\ g^{-1}$ for the Co–Fe catalyst.

Raman spectra of the fresh Co_3O_4 and Fe_2O_3 catalysts show characteristic peaks due to both oxides with bands at 484, 522, 620 and 690 cm^{-1} for Co_3O_4 [18,24] and 292, 410, 493 and 612 cm^{-1} for Fe_2O_3 [25,26] (Fig. 4). The Raman spectrum of the Co–Fe fresh catalyst showed peaks of Co_3O_4 with only very weak Fe_2O_3 features at 292 cm^{-1} observed which suggests that the Co_3O_4 could be covering the Fe phase in the Co–Fe sample. This is consistent with the observation by Casanovas et al. wherein, using HRTEM, they observed that in promoted Co/ZnO catalysts (1% Fe, Na, Cu, Cr or Ni), the Co-alloy particles were sometimes covered by Co_3O_4 [8].

The catalysts were pre-reduced in-situ in the catalytic testing prior to exposure to the reaction feed. To study the effect of the reduction on the oxides, temperature programmed reduction (TPR) was performed. Fig. 5 shows the TPR profiles for the Co_3O_4, Fe_2O_3 and Co–Fe catalysts. The reduction profile of Co_3O_4 contained two main peaks, one at 360 °C corresponding to the reduction of Co^{3+} to Co^{2+} and another at 473 °C corresponding to the reduction of Co^{2+} to Co^0 [27]. The reduction profile of Fe_2O_3 has three peaks, the first at 417 °C, the second at 636 °C and the third broad peak at ~835 °C. The first peak corresponds to the reduction of Fe_2O_3 to Fe_3O_4 while the second and the third peaks correspond to the transformation of Fe_3O_4 to Fe^0 which proceeds through FeO [28].

The reduction profile of the mixture Co–Fe, showed three main peaks at 350 °C, 460 °C and 660 °C with a small feature around 535 °C and a shoulder around 740 °C. The first peak corresponds to the reduction of Co^{3+} to Co^{2+}, which occurs at the same temperature as in the Co_3O_4 catalyst, while the other peaks are associated with overlapping features from the reduction of Co^{2+} to Co^0, Fe_2O_3 to Fe_3O_4 and Fe_3O_4 to Fe^0. The presence of Fe in the Co_3O_4 catalyst had little effect on the reduction temperature of Co species in contrast to supported Co/Al_2O_3 catalysts where addition of Fe enhanced Co reducibility [12]. In the case of the Co–Fe catalyst, TPR analysis showed that the reduction process was completed by ~775 °C

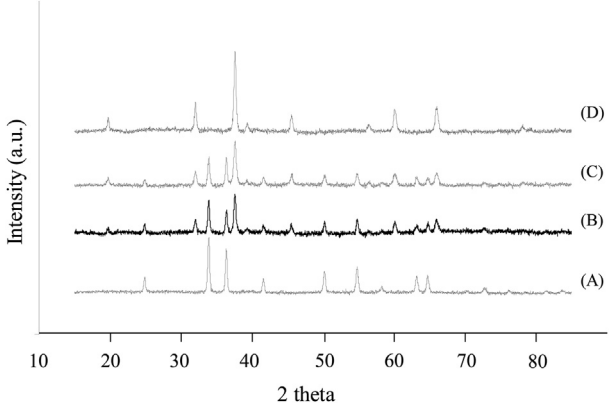

Fig. 2 – XRD patterns of Fe_2O_3 (A), Co–Fe-physical (B), Co–Fe (C) and Co_3O_4 (D).

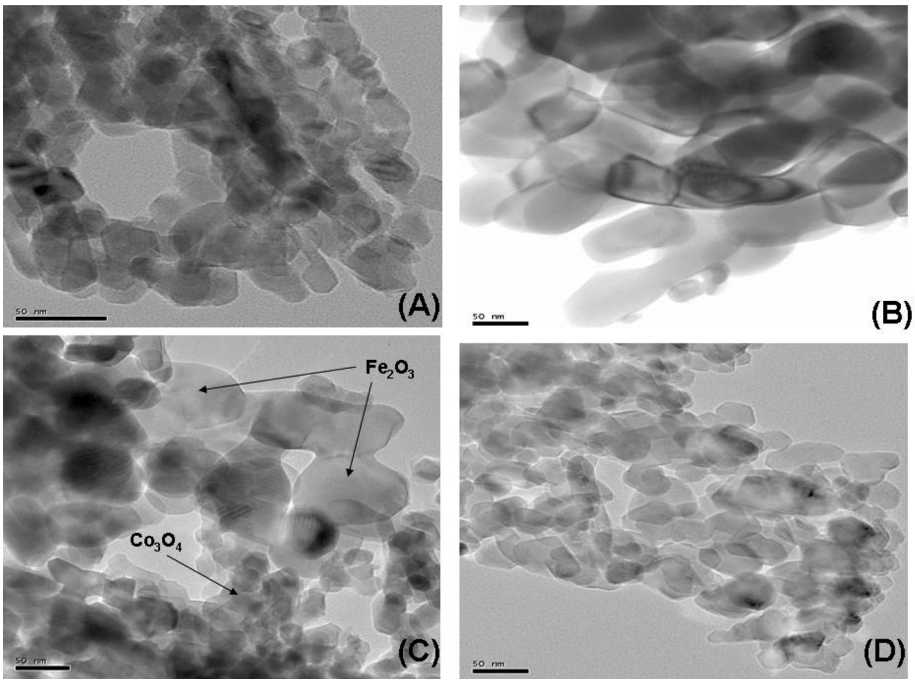

Fig. 3 – TEM photographs (scale 50 nm) for Co_3O_4 (A), Fe_2O_3 (B), Co–Fe-Physical (C) and Co–Fe (D) catalysts.

which is significantly lower than that found for pure Fe_2O_3 (985 °C) indicating a notable improvement in the reducibility of Fe_2O_3 in the mixture compared to the pure oxide. Increased reducibility of Co_3O_4 in the mixed sample aiding the higher temperature reduction of Fe_3O_4 to Fe metal has also been observed by Homs et al. [11] in iron promoted cobalt-based catalysts. However, TPR analysis of the Co–Fe catalyst reduction show that by 400 °C (the temperature used to activate catalyst prior to catalytic testing), the Co will be a mixture of Co_3O_4, CoO and, possibly, Co metal.

Characterisation of promoted Co catalysts suggests that addition of Fe improves the reduction of Co_3O_4 to Co^0 [12] and thus allows the catalyst to maintain an optimal balance between Co^0 and Co_3O_4 with Co_3O_4 reported to be the active phase for ethanol dehydrogenation and Co^0 for acetaldehyde reforming [8,16,29]. However, both CoO and Co^0 have been reported to co-exist in active ethanol steam reforming catalysts for both unsupported [16,17] and supported Co_3O_4 catalysts [30] with ease of exchange between metallic and oxidised cobalt suggested to be key for the activity. Following reduction at 400 °C, Fe would be present as Fe_2O_3 (possibly some Fe_3O_4); however, under the feed conditions, further reduction of Fe (and Co) could occur [31].

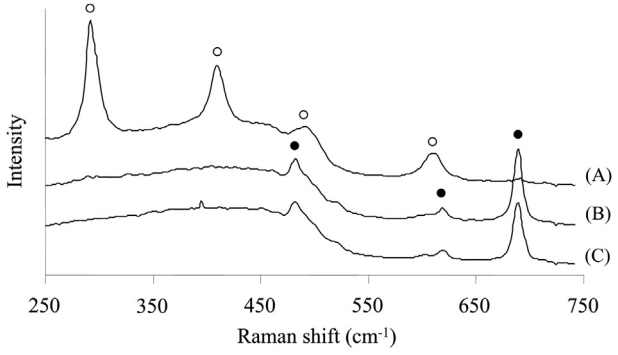

Fig. 4 – Raman spectra of fresh catalysts Fe_2O_3 (A), Co–Fe (B) and Co_3O_4 (C); bands due to Fe_2O_3 (●) and Co_3O_4 (○).

With rapid deactivation of the catalysts observed and the formation of undetected carbon, temperature programmed oxidation (TPO) of the catalysts after 2 h on stream at 500 °C was carried out (Fig. 5). Analysis of the CO_2 peak areas shows that the highest amount of CO_2 was formed from Co_3O_4 in comparison with the pure Fe_2O_3. The CO_2 peak positions in the TPO profiles of Co_3O_4 and Co–Fe are similar which suggests that the nature of the coke formed over these samples is not altered by the presence of Fe in Co–Fe. However, after 2 h of reaction, the amount of deposited coke on the Co_3O_4 is approximately three times higher that found on the Co–Fe sample which correlates well with the decrease in the undetected carbon in Table 1 and the relative deactivation profiles of the two catalysts. It should be noted that the Fe_2O_3 catalyst had the least amount of coke deposited and the peaks in the TPO profile occur at lower temperatures than found in the cobalt containing samples, i.e. showing the presence of more easily oxidisable coke.

Raman spectra of the used catalysts (recorded ex-situ after 15 h of reaction) are shown in Fig. 6. The used Co_3O_4 catalyst, showed no bands due to cobalt oxide species after reaction; however, two new bands at 1596 and 1310 cm^{-1} were observed and assigned to stretching mode of sp^2 carbon of ordered graphitic carbon (G band) and disordered carbon species (D band), respectively [10,32,33]. The spectrum of the Co–Fe used catalyst had the same graphitic bands (position and intensity) as observed over the Co_3O_4 catalyst which suggests that coke formation occurs on cobalt species rather than on Fe. The lack

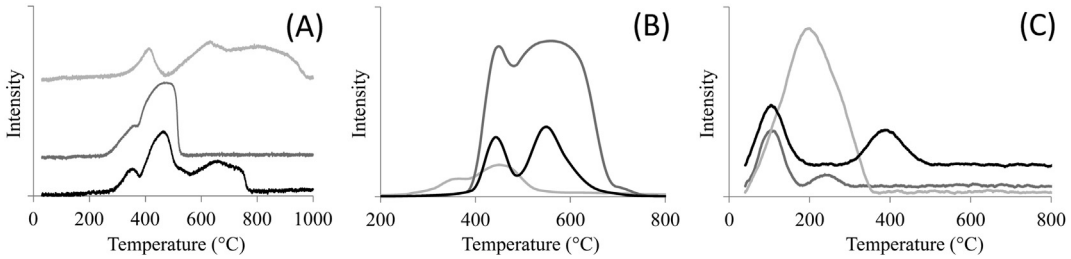

Fig. 5 – (A) TPR, (B) TPO after 2 h on stream at 500 °C under ethanol water feed (1:3 molar ratio) and (C) ammonia-TPD profiles of fresh Co_3O_4 (dark grey line), Fe_2O_3 (light grey line) and Co–Fe (black line) catalysts.

of bands due to cobalt oxide species suggest that either the coke is covering the cobalt or that the Co is reduced to Co^0 during reaction.

The Raman spectrum of the used Fe_2O_3 catalyst did not exhibit any bands due to Fe_2O_3 and no new bands were observed which suggests that any carbon laydown over this catalyst (undetected carbon in Table 1) is not graphitic but more likely from adsorbed ethoxy/acetate/carbonate species (see DRIFT spectra in Section 3.3). The Raman spectrum of the used Fe_2O_3 catalyst and the weak TPO profile suggests other deactivation processes to be the cause of the very rapid loss of activity observed over Fe_2O_3.

While Raman spectroscopy showed the same nature and amount of carbon formation on Co_3O_4 and Co–Fe samples, TPO analysis (and the amount of undetected carbon) showed the Co–Fe samples to have reduced coke formation compared with the Co_3O_4 catalyst. NH_3-TPD was performed to assess the concentration and strength of acidic sites on these catalysts. While NH_3-TPD can distinguish sites by sorption strength, it cannot differentiate between Brønsted and Lewis-acid sites [34]. In supported catalysts, basic supports are preferred in ethanol steam reforming as they do not favour ethanol dehydration to ethylene. According to Tanabe et al. [35] the strength of solid acid sites within TPD profiles can be classified by the temperature at which NH_3 desorbs with NH_3 desorbing from weak acid sites between 120 and 300 °C, moderate acid sites between 300 and 500 °C and strong acid sites between 500 and 650 °C.

NH_3-TPD profiles for Co_3O_4, Fe_2O_3 and Co–Fe fresh catalyst after reduction for 1 h at 400 °C are reported in Fig. 5. The NH_3-TPD profile of Fe_2O_3 exhibited one broad peak (40–340 °C) with a maximum at 200 °C. The broad nature of the peak indicates the presence of sites with a range of acid strength on this catalyst. For both Co_3O_4 and Co–Fe, the TPD profile contains two peaks, in the case of Co_3O_4 the peaks were at 104 °C and 240 °C, while in the case of Co–Fe the peaks were at 104 °C and 390 °C (with a third small feature at 240 °C) indicating the presence of two well defined acid sites in each case. The weak acid site corresponding to the peak at 104 °C is common to both samples and could be responsible for formation of the graphitic coke as detected by Raman spectroscopy. Following addition of Fe to the sample, the second peak at 240 °C which is observed over Co_3O_4 is depleted with the formation of new sites of moderate acidic strength (peak at 390 °C). The nature of the acid sites change upon addition of Fe_2O_3 to Co_3O_4 and consideration of the total acid site concentration from the area under the peaks, showed that the concentration of acid sites was greatest over Fe_2O_3 then Co–Fe and then Co_3O_4. Since the total number of acid sites does not follow the trend in the deactivation rate/amount of coke deposited on the catalyst, this suggests that specific sites are active for coke formation over the Co_3O_4 catalyst. The reduction of the peak at 240 °C following incorporation of Fe and lower coke deposition over this catalyst, suggests that loss of these acidic sites on the Co–Fe catalyst could be responsible for the reduced carbon laydown observed.

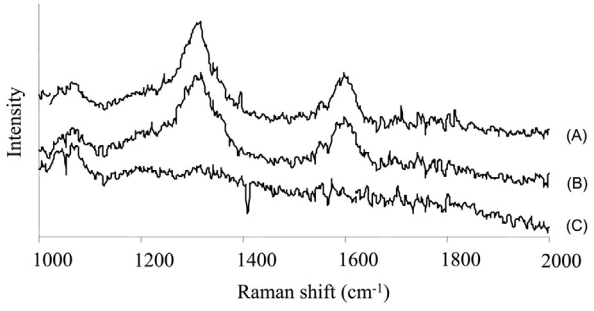

Fig. 6 – Raman spectra of catalysts after 15 h on stream at 500 °C under ethanol water feed (1:3 molar ratio) Co_3O_4 (A), Co–Fe (B) and Fe_2O_3 (C).

3.3. *DRIFTS-MS study*

The reaction network in the steam reforming of ethanol is complex with many reactions leading to intermediates and side products, such as ethylene, acetaldehyde, acetone, methane, ethane, and coke [21]. Co_3O_4, Fe_2O_3 and the Co–Fe catalysts exhibit differing activities and product selectivities for the steam reforming of ethanol with the Co–Fe catalyst exhibiting higher hydrogen yield with lower CH_4 and lower coke formation when compare with the Co_3O_4 catalyst (Table 1 and Fig. 1). In-situ DRIFTS-MS during a temperature ramp to 500 °C under the steam reforming feed over Co_3O_4, Fe_2O_3 and the Co–Fe samples was performed to probe the evolution of gas phase species whilst monitoring the surface adsorbed species to investigate the promotional effect of Fe_2O_3 on Co_3O_4.

For all three catalysts, 100% conversion of ethanol was achieved at 500 °C which is comparable to the results obtained in a plug flow reactor (Table 1 and Fig. 1) [36]. However, in the low temperature region (100–400 °C) the MS profiles over the three catalysts showed the formation of hydrogen (Fig. 7B), carbon oxides (Fig. 7C, D), ethylene (Fig. 7E), acetaldehyde (Fig. 7F), methane (Fig. 7G) and acetone (Fig. 7H) with the

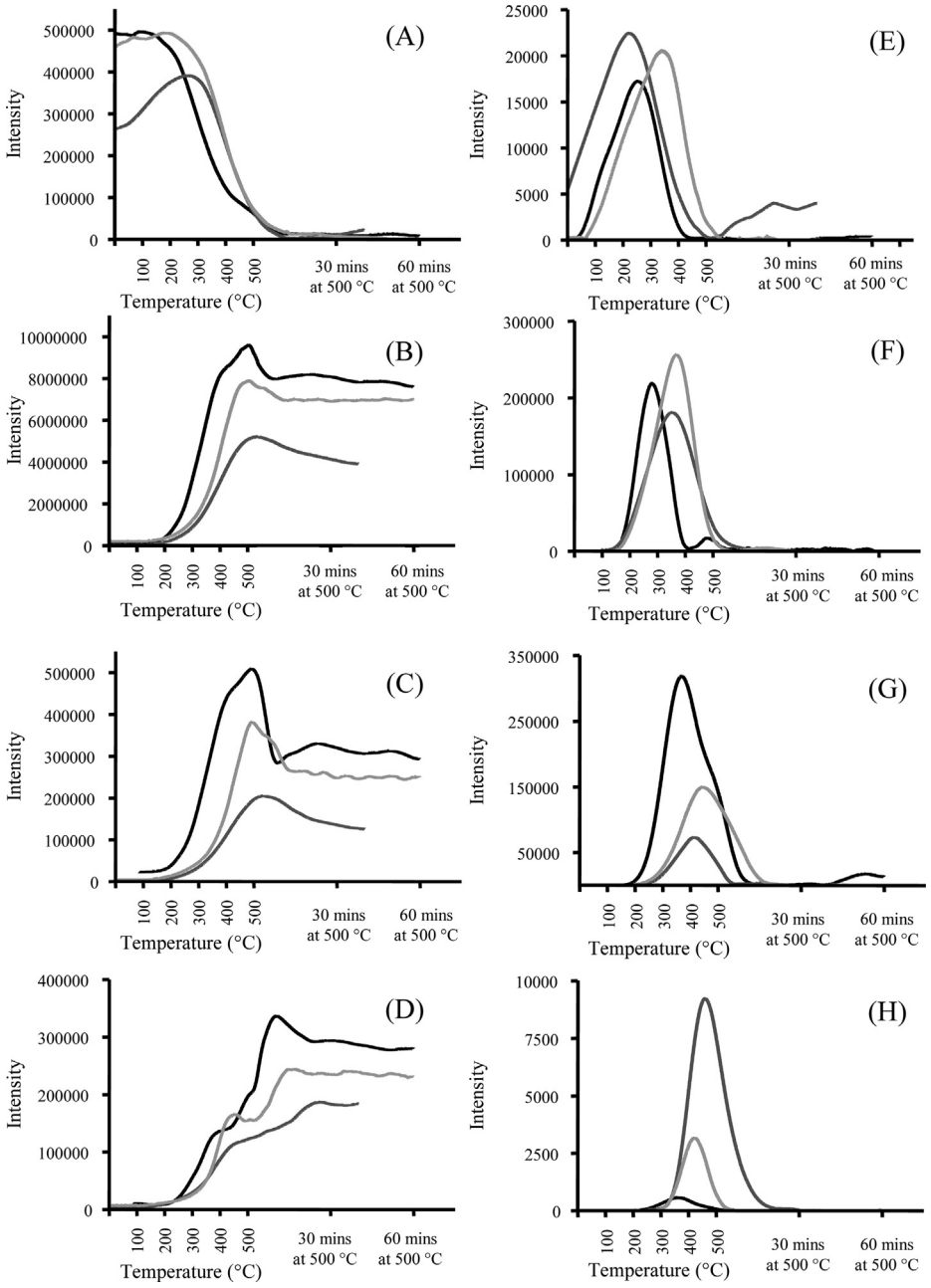

Fig. 7 – Reaction profile during temperature ramp from 100 °C to 500 °C and steady state at 500 °C under ethanol water feed (1:3 molar ratio) over Co_3O_4 (black line), Fe_2O_3 (grey line) and Co–Fe (light grey line) for conversion of ethanol (A), formation of H_2 (B), CO_2 (C), CO (D), ethylene (E), acetaldehyde (F), methane (G) and acetone (H).

relative proportions and temperature at which products/intermediates were formed found to vary with the catalyst.

Conversion of ethanol begins at a lower temperature over Co_3O_4, ~150 °C compared with ~280 °C for Fe_2O_3 and ~220 °C for Co–Fe (Fig. 7A). Initial low temperature formation of ethylene over Fe_2O_3 (upon switching to the feed at 100 °C) could be the cause of the initial higher ethanol conversion observed which recovers as the temperature increased.

While ethanol conversion begins at a lower temperature over Co_3O_4, between 400 and 500 °C the ethanol conversion profile changes exhibiting slower conversion at higher temperatures; this is not observed for Fe_2O_3 or the Co–Fe catalyst. The two stages of conversion of ethanol over Co_3O_4 is also evident in the product profiles which exhibit second peaks at higher temperatures.

Over Co-based catalysts, the ethanol steam reforming reaction pathway has been proposed to occur via the dehydrogenation of ethanol to acetaldehyde (Eq. (2)) followed by reforming of acetaldehyde in combination with the WGS reaction to form $CO_2 + H_2$ (Eq. (3)) with acetaldehyde proposed as the major intermediate [8]. Over Co_3O_4, Fe_2O_3 and Co–Fe catalysts, acetaldehyde began to be observed at ~150 °C (Fig. 7F); however, the temperature at which the maximum in acetaldehyde formation occurred varied from 270 °C over Co_3O_4 to

350 °C for Fe_2O_3 and 370 °C for the Co–Fe catalyst. Co_3O_4 was found to have the highest activity for the transformation of acetaldehyde. However, as the temperature increased from 400 to 500 °C, acetaldehyde was observed to form again (Fig. 7F). Over the Fe_2O_3 and Co–Fe catalysts acetaldehyde was still detected for the first ~10 min while at 500 °C.

Acetaldehyde can undergo decomposition reactions (Eq. (4)) as well as reforming reactions (Eq. (5)), with both pathways forming CO (which can react further to $CO_2 + H_2$ via WGS). Products from the transformation of acetaldehyde also include H_2 (via reforming) or methane (via decomposition). The amount of methane formed over the Co_3O_4 catalyst was significantly higher compared with the Fe_2O_3 catalyst (Fig. 7H). This is not consistent with previous reports where Co catalysts exhibited low methane formation under ethanol steam reforming conditions [37]. Co catalysts have also been reported to have low methanation activity at low to moderate temperatures [38] so it is likely that this methane found together with CO and H_2 comes via ethanol decomposition (Eq. (6)).

$$C_2H_5OH \rightarrow CH_3CHO + H_2 \quad (2)$$

$$CO + H_2O \rightarrow CO_2 + H_2 \quad (3)$$

$$CH_3CHO \rightarrow CH_4 + CO \quad (4)$$

$$CH_3CHO + H_2O \rightarrow 2CO + 3H_2 \quad (5)$$

$$C_2H_5OH \rightarrow CH_4 + CO + H_2 \quad (6)$$

The high selectivity towards methane over Co_3O_4 suggests that ethanol or acetaldehyde decomposition pathways are favoured compared with reforming reactions whereas over the Fe_2O_3 catalysts, the low methane suggests that reforming reactions are favoured. However, it was noted that the H_2 and CO_2 signals over Fe_2O_3 decrease over the 1 h period at 500 °C (Fig. 7B and C). Although Fe_2O_3 catalysts form less methane they are not as active as the Co_3O_4 (or Co–Fe) catalysts and exhibit rapid deactivation (Fig. 1).

Acetone, a minor product, was also formed during the temperature ramp to 500 °C over the three catalysts with the maximum amount of acetone in the gas phase observed at 470 °C over Fe_2O_3, 370 °C over Co_3O_4 and 430 °C for the Co–Fe catalyst (Fig. 7H). The onset in acetone formation is observed at the temperature where acetaldehyde begins to react for all catalysts which suggests that the acetone comes from reaction of acetaldehyde. It has been proposed that acetone can form from the aldol condensation reaction of two acetaldehyde molecules [39]. The differing amounts of acetone formed over the Co_3O_4 and Fe_2O_3 catalysts highlights the different reactions of acetaldehyde occurring over the two catalysts. Over Co_3O_4 decomposition or reforming of acetaldehyde occurs while over Fe_2O_3, which has low C–C bond breaking activity, aldol condensation of acetaldehyde is the more significant reaction.

As well as dehydrogenation of ethanol to acetaldehyde, dehydration to ethylene can also occur as an unwanted side reaction leading to coke formation. The temperature at which the maximum in the formation of ethylene occurs is higher over Co–Fe compared with Co_3O_4 or Fe_2O_3 oxides alone. The change in activity for ethylene conversion could be responsible for the reduced coke formation observed over the mixed metal catalyst (Table 1).

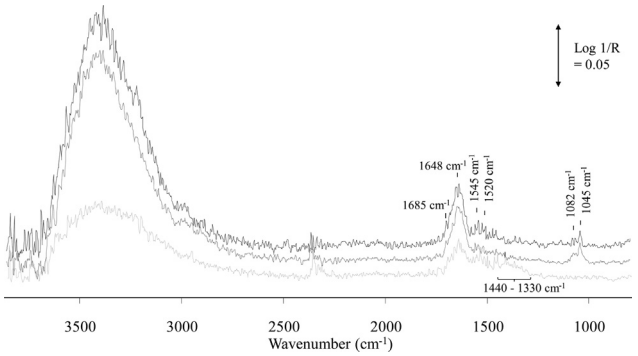

Fig. 8 – DRIFT spectra recorded at 100 °C: Fe_2O_3 (dark grey spectrum), Co–Fe (black) and Co_3O_4 (light grey spectrum) under ethanol/water feed (1:3 molar ratio). Catalysts were pre-reduced at 400 °C under H_2 and cooled to 100 °C before introduction of the feed. Spectra have been corrected for contributions due to gas phase ethanol.

Fig. 8 shows DRIFT spectra of Co_3O_4 and Fe_2O_3 at 100 °C under the ethanol/water feed referenced to the respective reduced catalysts before exposure to the feed. On the Fe_2O_3 catalyst under the feed at 100 °C, bands due to adsorbed water (bands between 3700–3000 and 1646 cm^{-1}), acetyl species, a band at 1685 cm^{-1} (shoulder to higher wavenumber of the 1646 cm^{-1} which can form from dehydrogenation of acetaldehyde) [40] and ethoxy species, bands at 1082 and 1045 cm^{-1}, were observed [29,41]. Bands due to acetate species were also observed at 1545 and carbonates at 1525 cm^{-1} [40]. The Co_3O_4 spectrum at 100 °C has similar adsorbed species to Fe_2O_3 with water, acetyl and acetate species observed. The major difference between the Co_3O_4 and Fe_2O_3 catalysts is the lack of ethoxy bands on the Co_3O_4 and the presence of additional, although weak, acetate bands between 1450 and 1330 cm^{-1} which suggests that ethanol adsorbs and is oxidised to acetate on Co_3O_4 at low temperatures. While comparable species are observed on the Fe_2O_3 and Co_3O_4 catalysts, the relative intensity of the adsorbed water to acetate bands varied significantly with the water/OH bands observed over the Fe catalyst at 100 °C being significantly more intense compared with the acetate/carbonate bands while for the Co_3O_4 catalyst, these bands are of more comparable intensities (Fig. 8). The DRIFT spectrum of the Co–Fe catalyst resembles the spectrum of Fe_2O_3 at 100 °C (Fig. 8) with comparable relative intensities of the adsorbed water and ethoxy bands.

On ramping the temperature to 500 °C under the ethanol/water feed, the ethoxy/acetate species and water/OH surface coverage decrease over all catalysts although at differing rates which is in line with the MS results where different temperature ranges for the formation/reaction of intermediates/by-products was observed over the catalysts.

Over Fe_2O_3, as the temperature increases, there was an initial increase in the intensity of the water and ethoxy bands up to a temperature of 200 °C (Fig. 9). Above 200 °C, bands due

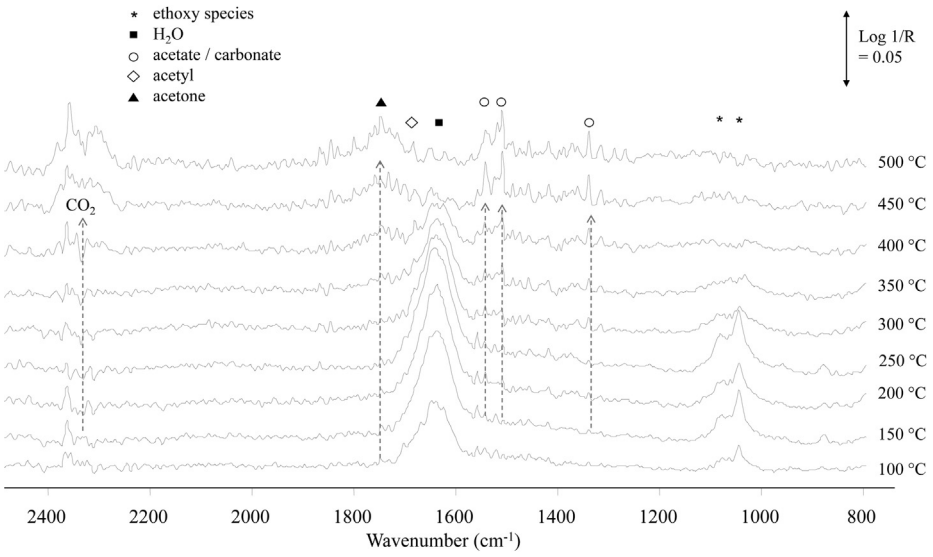

Fig. 9 – DRIFT spectra of Fe_2O_3 under ethanol/water feed (1:3 molar ratio) from 100 to 500 °C (heating rate 10 °C min^{-1}). Grey arrows highlight species which grow with increasing temperature.

to water and ethoxy species began to decrease with further increases in temperature with ethoxy bands no longer observed above 350 °C and water bands no longer observed above 400 °C. At 400 °C, a new band is observed at 1743 cm^{-1} which could be due to the formation of acetaldehyde or acetone (υ(C═O)). Other bands to aid the assignment were not distinguishable and hence unambiguous assignment from the DRIFT spectra was not possible. This new band, however, increases in intensity up to a temperature of 500 °C over Fe_2O_3 after which it remains constant. Once this species is formed, it is strongly adsorbed on the catalyst surface. The temperature at which the 1743 cm^{-1} band is observed corresponds with the reaction of acetaldehyde to form acetone; temperature at which the maximum acetaldehyde is formed in the gas phase (Fig. 7). Using TPD experiments of acetaldehyde and acetone adsorbed over Co/ZrO_2 and Co/CeO_2 catalysts, Song et al. showed that acetone had a stronger interaction with the surface; products from acetone conversion were also observed over a much greater temperature range than acetaldehyde [39]. Most of the acetaldehyde desorption features were in the temperature range of 300–350 °C while with acetone, products were formed between 250 and 550 °C. This suggests that the band at 1743 cm^{-1} could be due to acetone strongly adsorbed on the catalyst surface. As well as the band at 1743 cm^{-1}, as the temperature increases, the bands at 1541, 1458 and 1345 cm^{-1} due to acetate/carbonate species increase. At 500 °C, the Fe_2O_3 catalyst surface has adsorbed acetone and acetate/carbonate species.

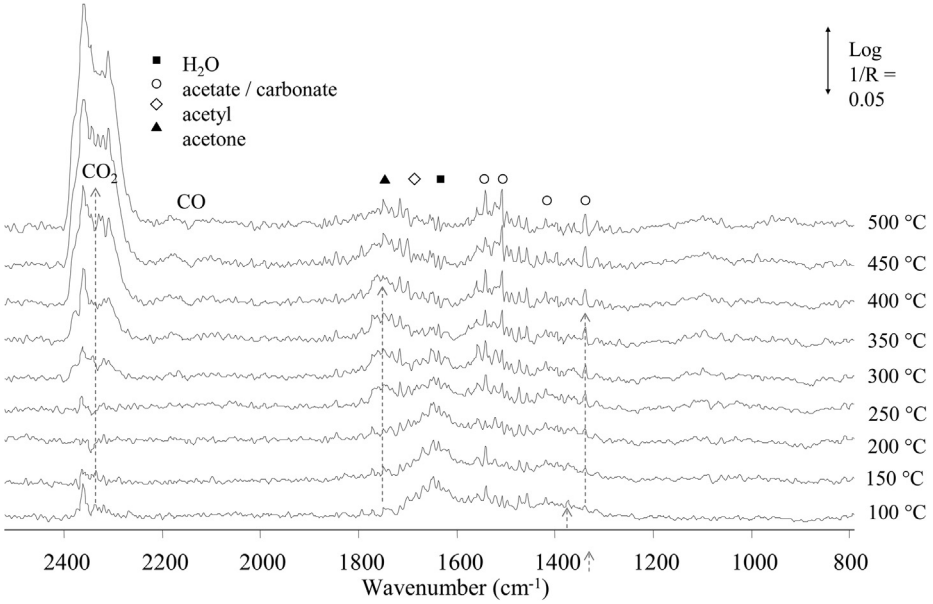

Fig. 10 – DRIFT spectra of Co_3O_4 under ethanol/water feed (1:3 molar ratio) from 100 to 500 °C (heating rate 10 °C min^{-1}). Grey arrows highlight species which grow with increasing temperature.

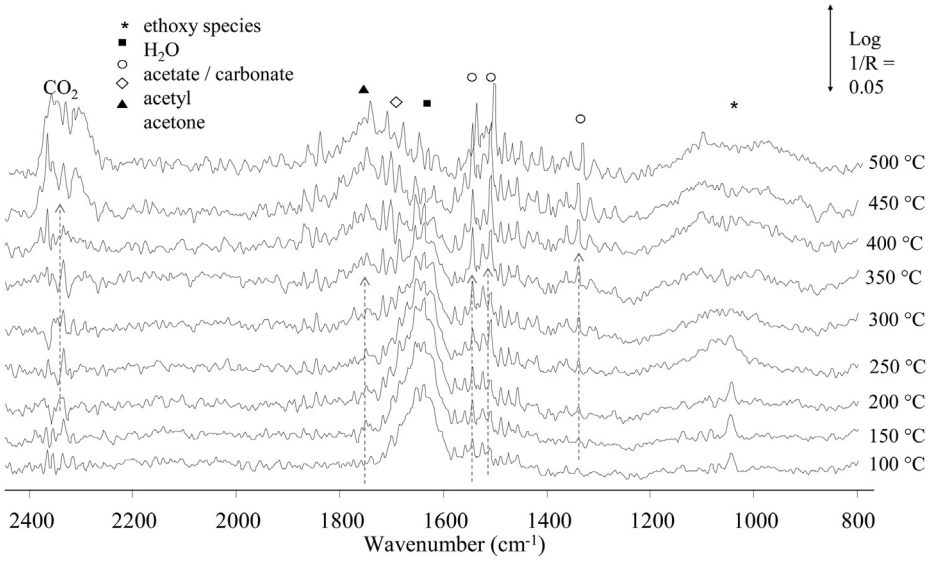

Fig. 11 – DRIFT spectra of Co–Fe under ethanol/water feed (1: 3 molar ratio) from 100 to 500 °C (heating rate 10 °C min^{-1}). Grey arrows highlight species which grow with increasing temperature.

Over Co_3O_4, at 100 °C, water/OH bands and acetyl bands are much weaker than over Fe_2O_3 and no ethoxy bands were observed (Fig. 10). No change in the adsorbed species occurred between 100 and 200 °C. The bands due to adsorbed water began to decrease above 250 °C and were no longer observed above 350 °C; 100 °C lower than over the Fe_2O_3 catalyst. MS data for the conversion of ethanol with increasing temperature profile (Fig. 7A) showed a decrease in the ethanol conversion rate between 400 and 500 °C which corresponds with the temperature range where water is no longer adsorbed on the Co_3O_4 catalyst. This suggests that with the increasing temperature, the extent of conversion of ethanol through reforming and decomposition reactions could be altered with decomposition becoming more significant at higher temperature when water/OH is no longer adsorbed on the catalyst.

Over Co_3O_4 at 250 °C, (as opposed to 400 °C for the Fe_2O_3 catalyst) a band at 1745 cm^{-1} assigned to acetone was observed. This band increases slightly at 300 °C and then remains constant, decreasing above 450 °C to a weak band which is still present at 500 °C. Co_3O_4 has a higher activity than Fe_2O_3 for transformation of acetone. Co_3O_4 catalyst also shows a decrease in acetate/carbonate bands with increasing temperature and like Fe_2O_3, at 500 °C, has only bands due to acetone and acetate/carbonate species.

DRIFT spectra of the Co–Fe catalyst under ethanol/water with increasing temperature are shown in Fig. 11. The DRIFT spectrum of Co–Fe at 100 °C has the same water and ethoxy bands as the Fe_2O_3 catalyst (Fig. 8). As the temperature is ramped to 500 °C the following changes are observed:

(i) water/OH bands initially increase in intensity with increasing temperature and are no longer observed at 450 °C as for the Fe_2O_3 catalyst;
(ii) ethoxy bands are no longer observed by 300 °C which is at a lower temperature compared to Fe_2O_3 (350 °C);
(iii) at 350 °C, the band associated with acetone formation (1745 cm^{-1} band) is detected which is at an intermediate temperature between Co_3O_4 (250 °C) and Fe_2O_3 400 °C;
(iv) acetone and acetate/carbonate species are present on all three catalysts at 500 °C under the feed.

Interestingly, coke formation from the build up of acetate/carbonate species has been proposed over catalysts under the ESR conditions; [42] however all the catalysts have comparable intensity bands due to acetate/carbonate bands at 500 °C with very different amounts/nature of carbon deposited (Table 1). The higher H_2 yield over the Co–Fe catalyst compared with the pure oxides may be related to the increase in water/OH species adsorbed on the catalyst at lower temperatures. The higher concentration of OH species on the Co phase in Co–Fe would favour reforming activity rather than decomposition reactions which are favoured over the pure Co_3O_4 catalyst at these temperatures therefore increasing the selectivity to H_2 over methane, for example.

4. Conclusions

The Co–Fe sample exhibited not only higher H_2 yield but also reduced by-product formation compared with the pure oxides and the physical mixture. The DRIFT-MS study highlighted that properties of the individual oxides were maintained in the Co–Fe catalyst in particular the adsorption properties of Fe_2O_3 (water/OH present on the catalyst to higher temperatures) which is a result of the preparation method used; formation of separate cobalt and iron phases in intimate contact. Increasing the amount of reactive species (higher ratio of water to ethoxy/acetate species at higher temperatures) adsorbed on the Co–Fe catalyst surface compared with the Co_3O_4 catalyst is proposed to facilitate reforming over decomposition reactions reducing by-product formation and providing a higher H_2 yield.

Acknowledgements

The authors would like to thank Mr. Stephen McFarland at QUB School of Mathematics and Physics for assistance with TEM and EDX measurements and the Egyptian government and the CASTech grant (EP/G012156/1) from the EPSRC for financial support.

REFERENCES

[1] Barbir F. Transition to renewable energy systems with hydrogen as an energy carrier. Energy 2009;34:308–12.
[2] Ni M, Leung DYC, Leung MKH. A review on reforming bio-ethanol for hydrogen production. International Journal of Hydrogen Energy 2007;32:3238–47.
[3] Haryanto A, Fernando S, Murali N, Adhikari S. Current status of hydrogen production techniques by steam reforming of ethanol: a review. Energy & Fuels 2005;19:2098–106.
[4] Sekine Y, Kazama A, Izutsu Y, Matsukata M, Kikuchi E. Steam reforming of ethanol over cobalt catalyst modified with small amount of iron. Catalysis Letters 2009;132:329–34.
[5] Profeti LPR, Ticianelli EA, Assaf EM. Production of hydrogen by ethanol steam reforming on Co/Al_2O_3 catalysts: effect of addition of small quantities of noble metals. Journal of Power Sources 2008;175:482–9.
[6] Profeti LPR, Ticianelli EA, Assaf EM. Ethanol steam reforming for production of hydrogen on magnesium aluminate-supported cobalt catalysts promoted by noble metals. Applied Catalysis A: General 2009;360:17–25.
[7] Torres JA, Llorca J, Casanovas A, Domínguez M, Salvadó J, Montané D. Steam reforming of ethanol at moderate temperature: multifactorial design analysis of Ni/La_2O_3–Al_2O_3, and Fe- and Mn-promoted Co/ZnO catalysts. Journal of Power Sources 2007;169:158–66.
[8] Casanovas A, Roig M, de Leitenburg C, Trovarelli A, Llorca J. Ethanol steam reforming and water gas shift over Co/ZnO catalytic honeycombs doped with Fe, Ni, Cu, Cr and Na. International Journal of Hydrogen Energy 2010;35:7690–8.
[9] Homs N, Llorca J, de la Piscina PR. Low-temperature steam-reforming of ethanol over ZnO-supported Ni and Cu catalysts: the effect of nickel and copper addition to ZnO-supported cobalt-based catalysts. Catalysis Today 2006;116:361–6.
[10] Llorca J, Homs N, Sales J, Fierro J-LG, Ramírez de la Piscina P. Effect of sodium addition on the performance of Co–ZnO-based catalysts for hydrogen production from bioethanol. Journal of Catalysis 2004;222:470–80.
[11] de la Peña O'Shea VA, Nafria R, Ramírez de la Piscina P, Homs N. Development of robust Co-based catalysts for the selective H_2-production by ethanol steam-reforming. The Fe-promoter effect. International Journal of Hydrogen Energy 2008;33:3601–6.
[12] Huang L, Chen R, Chu D, Hsu AT. Hydrogen production through auto-thermal reforming of bio-ethanol over Co-based catalysts: effect of iron in Co/Al_2O_3 catalysts. International Journal of Hydrogen Energy 2010;35:1138–46.
[13] Natile MM, Poletto F, Galenda A, Glisenti A, Montini T, Rogatis LD, et al. $La_{0.6}Sr_{0.4}Co_{1-y}Fe_yO_{3-\delta}$ perovskites: influence of the Co/Fe atomic ratio on properties and catalytic activity toward alcohol steam-reforming. Chemistry of Materials 2008;20:2314–27.
[14] Kazama A, Sekine Y, Oyama K, Matsukata M, Kikuchi E. Promoting effect of small amount of Fe addition onto Co catalyst supported on [alpha]-Al_2O_3 for steam reforming of ethanol. Applied Catalysis A: General 2010;383:96–101.
[15] Lin SSY, Kim DH, Ha SY. Metallic phases of cobalt-based catalysts in ethanol steam reforming: the effect of cerium oxide. Applied Catalysis A: General 2009;355:69–77.
[16] Llorca J, Ramírez de la Piscina P, Dalmon J-A, Homs N. Transformation of Co_3O_4 during ethanol steam-re-forming. activation process for hydrogen production. Chemistry of Materials 2004;16:3573–8.
[17] de la Peña O'Shea VA, Homs N, Pereira EB, Nafria R, Ramírez de la Piscina P. X-ray diffraction study of Co_3O_4 activation under ethanol steam-reforming. Catalysis Today 2007;126:148–52.
[18] Wang C-B, C–C Lee, Bi J-L, Siang J-Y, Liu J-Y, Yeh C- T. Study on the steam reforming of ethanol over cobalt oxides. Catalysis Today 2009;146:76–81.
[19] Gabal MA, El-Bellihi AA, Ata-Allah SS. Effect of calcination temperature on Co(II) oxalate dihydrate-iron(II) oxalate dihydrate mixture: DTA-TG, XRD, Mossbauer, FT-IR and SEM studies (part II). Materials Chemistry and Physics 2003;81:84–92.
[20] Meunier FC, Goguet A, Shekhtman S, Rooney D, Daly H. A modified commercial DRIFTS cell for kinetically relevant operando studies of heterogeneous catalytic reactions. Applied Catalysis A: General 2008;340:196–202.
[21] Llorca J, Homs N, Sales J, de la Piscina PR. Efficient production of hydrogen over supported cobalt catalysts from ethanol steam reforming. Journal of Catalysis 2002;209:306–17.
[22] Tang C-W, Wang C-B, Chien S- H. Characterization of cobalt oxides studied by FT-IR, Raman, TPR and TG-MS. Thermochimica Acta 2008;473:68–73.
[23] Delille F, Dieny B, Moussy JB, Guittet MJ, Gota S, Gautier-Soyer M, et al. Study of the electronic paraprocess and antiphase boundaries as sources of the demagnetisation phenomenon in magnetite. Journal of Magnetism and Magnetic Materials 2005;294:27–39.
[24] Batista MS, Santos RKS, Assaf EM, Assaf JM, Ticianelli EA. Characterization of the activity and stability of supported cobalt catalysts for the steam reforming of ethanol. Journal of Power Sources 2003;124:99–103.
[25] de Faria DLA, Venâncio Silva S, de Oliveira MT. Raman microspectroscopy of some iron oxides and oxyhydroxides. Journal of Raman Spectroscopy 1997;28:873–8.
[26] Schlueter C, Lübbe M, Gigler AM, Moritz W. Growth of iron oxides on Ag(111) – reversible Fe_2O_3/Fe_3O_4 transformation. Surface Science 2011;605:1986–93.
[27] Xue L, Zhang C, He H, Teraoka Y. Catalytic decomposition of N_2O over CeO_2 promoted Co_3O_4 spinel catalyst. Applied Catalysis B: Environmental 2007;75:167–74.
[28] Liang M, Kang W, Xie K. Comparison of reduction behavior of Fe_2O_3, ZnO and $ZnFe_2O_4$ by TPR technique. Journal of Natural Gas Chemistry 2009;18:110–3.
[29] Llorca J, Homs N, Ramirez de la Piscina P. In situ DRIFT-mass spectrometry study of the ethanol steam-reforming reaction over carbonyl-derived Co/ZnO catalysts. Journal of Catalysis 2004;227:556–60.
[30] Llorca J, Dalmon J-A, Ramírez de la Piscina P, Homs N. In situ magnetic characterisation of supported cobalt catalysts under steam-reforming of ethanol. Applied Catalysis A: General 2003;243:261–9.
[31] Rosmaninho MG, Moura FCC, Souza LR, Nogueira RK, Gomes GM, Nascimento JS, et al. Investigation of iron oxide reduction by ethanol as a potential route to produce hydrogen. Applied Catalysis B: Environmental 2012;115-116:45–52.
[32] Cai W, Piscina PRDL, Homs N. Hydrogen production from the steam reforming of bio-butanol over novel supported Co-

based bimetallic catalysts. Bioresource Technology 2012;107:482–6.
[33] Song H, Ozkan US. Ethanol steam reforming over Co-based catalysts: role of oxygen mobility. Journal of Catalysis 2009;261:66–74.
[34] Hosseinpour N, Mortazavi Y, Bazyari A, Khodadadi AA. Synergetic effects of Y-zeolite and amorphous silica-alumina as main FCC catalyst components on triisopropylbenzene cracking and coke formation. Fuel Processing Technology 2009;90:171–9.
[35] Tanabe K, Misono M, Ono Y, Hattori H. Determination of acidic and basic properties on solid surfaces. Studies in surface science and catalysis. Elsevier; 19895–25.
[36] Meunier FC. The design and testing of kinetically-appropriate operando spectroscopic cells for investigating heterogeneous catalytic reactions. Chemical Society Reviews 2010;39:4602–14.
[37] Llorca J, Casanovas A, Trifonov T, Rodríguez A, Alcubilla R. First use of macroporous silicon loaded with catalyst film for a chemical reaction: a microreformer for producing hydrogen from ethanol steam reforming. Journal of Catalysis 2008;255:228–33.
[38] Casanovas A, de Leitenburg C, Trovarelli A, Llorca J. Catalytic monoliths for ethanol steam reforming. Catalysis Today 2008;138:187–92.
[39] Song H, Bao X, Hadad C, Ozkan U. Adsorption/desorption behavior of ethanol steam reforming reactants and intermediates over supported cobalt catalysts. Catalysis Letters 2011;141:43–54.
[40] de Lima SM, da Silva AM, da Costa LOO, Assaf JM, Jacobs G, Davis BH, et al. Evaluation of the performance of Ni/La_2O_3 catalyst prepared from $LaNiO_3$ perovskite-type oxides for the production of hydrogen through steam reforming and oxidative steam reforming of ethanol. Applied Catalysis A: General 2010;377:181–90.
[41] Song H, Mirkelamoglu B, Ozkan US. Effect of cobalt precursor on the performance of ceria-supported cobalt catalysts for ethanol steam reforming. Applied Catalysis A: General 2010;382:58–64.
[42] Virginie M, Araque M, Roger A-C, Vargas JC, Kiennemann A. Comparative study of H_2 production by ethanol steam reforming on $Ce_2Zr_{1.5}Co_{0.5}O_{8-\delta}$ and $Ce_2Zr_{1.5}Co_{0.47}Rh_{0.07}O_{8-\delta}$: evidence of the Rh role on the deactivation process. Catalysis Today 2008;138:21–7.